

A Dayem Loop Qubit Based on Interfering Superconducting Nanowires

Cliff Sun and Alexey Bezryadin

Department of Physics, University of Illinois at Urbana-Champaign

(*Electronic mail: bezryadi@illinois.edu)

(*Electronic mail: cliffxs2@illinois.edu)

We propose a qubit design based on two parallel superconducting nanowires (i.e., a "Dayem loop qubit"). The inclusion of two nanowires instead of one leads to the Little-Parks effect, which provides an oscillator behavior for the qubit frequency as well as anharmonicity. Our key result is that even if the nanowires have an increasingly linear CPR at low supercurrents, the quantum interference between two condensates, induced by a magnetic field, leads to a restoration of cubic nonlinearity, which is predicted to be sufficient to create a functional transmon qubit based on thin superconducting wires. We consider both generic (cubic) current-phase relationships (CPR) as well as more realistic microscopic CPR, having higher-order nonlinearities. For higher-order CPRs, we propose a simple power-law phenomenological approximation valid at very low temperatures, at which superconducting qubits normally operate.

I. INTRODUCTION

Quantum information processing has seen a rapid surge in interest due to its potential for dramatic speed-ups in optimization tasks^{1,2} and its ability to efficiently simulate high-dimensional quantum systems. Many major technology companies such as Microsoft, IBM, and Amazon are actively developing quantum computing resources, driving the need for scalable and robust quantum hardware.

Among the leading qubit architectures, superconducting qubits have emerged as the popular architecture for scalable quantum computing, but their reliance on millikelvin temperatures limits scalability^{3,4}. Devices capable of operating above 1 Kelvin could eliminate the need for dilution refrigerators and enable more practical large-scale systems. A key obstacle is the aluminum-based qubits used in most current quantum circuits. The small superconducting gap of aluminum restricts operation to below ~ 200 mK, where Bogoliubov quasiparticles cause significant decoherence⁵.

Conventional metal–oxide–metal junctions (SIS junctions) also introduce parasitic capacitance, limiting the qubit operation frequency. High-temperature operation requires much higher frequencies to suppress thermal excitations. However, as the operating frequency is increased, the dielectric losses in the oxide barrier also increase, further reducing coherence times.

Several alternative strategies have been explored to overcome these constraints. One direction enhances conventional aluminum junctions by proximitizing them with higher-gap superconductors, such as niobium, thereby extending operation toward 1 Kelvin⁶. A different route replaces aluminum-based elements entirely with nitride platforms, for example, NbN/AlN/NbN tunnel junctions⁷ or TiN nanowires⁸ acting as phase-slip junctions⁹, which inherently support higher-gap superconductivity and improved thermal robustness. Yet another approach introduced recently relies on superconductor-insulator quantum transition in NbN films¹⁰.

Here we develop an alternative idea, namely a fully metallic qubit that does not involve tunnel barriers, superconductor-semiconductor interfaces, quantum phase slips, or superconductor-insulator transitions. Our proposal is based on the superconducting quantum interference

between two homogeneous fully metallic superconducting nanowires^{11–15}, whose length L is larger than its superconducting coherence length ξ . Unlike in tunnel junctions, the supercurrent in the nanowire does not flow through a lossy amorphous oxide; thereby, a major source of decoherence can be eliminated¹⁶. Moreover, superconducting nanowires can be fabricated with diameters of only a few nanometers^{17,18} and possess a high kinetic inductance^{11,19}, making them attractive for realizing sub-micron superconducting circuits. Also, the electric capacitance of a nanowire transmon qubit is much smaller than in traditional transmon based on SIS junctions since the distance between the superconducting banks (antennas) of the qubit equals the length of the wire, which is typically of the order of 100 nm or larger.

Models of single nanowire qubits have previously been reported^{15,20}. It was suggested that such qubits can operate in the W-band (75–110 GHz), thereby reducing the risk of decoherence and quasiparticle-induced thermodynamic fluctuations¹⁵. Theoretically, single nanowire qubits can achieve an anharmonicity similar to a tunnel junction transmon qubit²⁰. But a major limitation of the single nanowire design is that its kinetic inductance becomes highly nonlinear only at high supercurrents, whereas traditional transmon qubits are biased at low supercurrents, representing just one quantum of energy. These nanowires resemble Dayem bridges in the sense that they do not have any barriers and yet act as weak superconducting links because of the constriction of the condensate to a very narrow channel, practically of the order of 10 nm^{17,18,21}. Nonlinear effects can also be increased by making bilayer nanowires, which include normal metals driven superconducting by the proximity effect²².

Here we demonstrate that the nonlinearity can be drastically increased if two nanowires are connected in parallel and a phase shift is generated between them by a magnetic field. Thus we propose a qubit design composed of two parallel superconducting nanowires forming a superconducting quantum interference device (SQUID), i.e., a nanowire-based SQUID. We demonstrate that this architecture provides sufficient intrinsic nonlinearity to achieve the anharmonicity required for practical qubit operation.

Initially, we analyze this system using a simplified generic model of the qubit CPR (termed "Likharev CPR" from

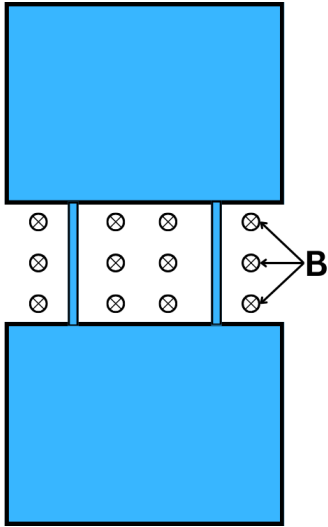


FIG. 1. **Schematic of a Dayem loop qubit.** It involved two superconducting thin-film electrodes connected by two parallel nanowires, which are assumed identical. The electrodes form a coplanar capacitor C . The magnetic field B is applied perpendicular to the device, as shown by the circles with "x" symbols in them.

Ref.²³). Two main conclusions follow from this analysis. (1) If the critical current of the wire is too large (in practice, this is usually the case) and the corresponding frequency of the resulting transmon is too high, then it is always possible to reduce the qubit frequency by increasing the wire inductance by making the nanowires longer, since the inductance is linearly proportional to the length. (2) As the magnetic field is increased, the phase shift between the wires increases proportionally. This leads to a reduction of the linear inductance of the device while the nonlinear inductance remains unchanged. Therefore, the relative anharmonicity increases with magnetic field as a Lorentzian function and diverges as the critical current of the device goes to zero.

We also study a more realistic CPR, previously predicted by microscopic theory calculations²⁰. We demonstrate that such zero-temperature CPR can be approximated by a simple power-law formula, which we use to analyze the anharmonicity of Dayem loop qubits. For the higher-power nonlinearity, the main conclusions are as follows. (1) The qubit frequency can still be adjusted by changing the wire length, since the linear term in the kinetic inductance is proportional to the wire length in any scenario. (2) At zero magnetic field, the nonlinear cubic term is absent, so the anharmonicity is probably too small for practical qubits. (3) At non-zero magnetic fields, a cubic term appears in the CPR of the device, and then the absolute anharmonicity can be increased by increasing the magnetic field. The relative anharmonicity shows an even stronger increase with the magnetic field, compared with the simplified cubic-nonlinearity CPR.

II. STRUCTURE OF THE DAYEM LOOP QUBIT

A schematic of the Dayem loop qubit is shown in Fig. 1. For simplicity, we always assume that the nanowires are identical to each other. Two nanowires are connected, in parallel, to larger electrodes (blue rectangles). These electrodes play the role of antennas (if the device is measured within a 3D microwave cavity) and also play the role of a shunting capacitor C , which impacts the energy levels of the qubit as well as its anharmonicity and the Coulomb charging energy $E_c = e^2/2C$ (e is the absolute value of the single-electron charge). Generally speaking, a transmon qubit can be viewed as an anharmonic oscillator, in which the oscillations arise from the back-and-forth flow of superconducting condensate electrons between the electrodes through the nanowires, acting as weak links between the electrodes. The analogy between the anharmonic oscillator and the transmon qubit is further explored in Appendix A. The design discussed here is similar to the traditional transmon qubit design²⁴, but the nanowires provide the weak links. We envision that nanowires would be on the order of 100 nm in length and ~ 10 nm in diameter, and the electrodes would be on the order of 100-500 μm in lateral dimension, and the thickness would be, say, 100 nm, as in Ref.¹¹. The critical current of each nanowire might be of the order of 1 μA , as in, e.g., DNA-based nanowires¹⁸.

The device is placed in a magnetic field perpendicular to the device plane (Fig. 1). This magnetic field creates a phase difference between the wires and a persistent bias current in the wires. The phase difference of wire "2" (the right wire) is related to the phase difference of wire "1" as $\phi_2 = \phi_1 + 2\pi b$, assuming that there are no trapped vortices in the device²⁵. This phase shift is created and defined by the Meissner currents in the electrodes¹⁸. This formula assumes that the phase gradients in the electrodes (antennas) do not depend on the current in the wires but only depend on the Meissner currents in the antennas themselves. In this formula, b is the normalized magnetic field defined as $b = B/\Delta B$, where B is the applied magnetic field and ΔB is the periodicity of the superconducting quantum interference device (SQUID), created by the two parallel nanowires.

Below, we will consider two models for this device. The first model, simplified, is based on Ginzburg-Landau (GL) perturbation theory, and the second, more realistic model will be based on the zero-temperature current-phase relationship (CPR) obtained by solving Usadel equations and reported previously in Ref.²⁰.

III. SIMPLIFIED DAYEM LOOP QUBIT MODEL

A. Current-Phase Relationship

In this section, we consider a simplified nanowire current-phase relationship (CPR) derived from the GL theory in Appendix B. Such a CPR will be referred to as the "Likharev CPR"²³ and is given as:

$$I(\phi) = \frac{3}{2} I_c \left[\frac{\phi}{\phi_c} - \frac{1}{3} \frac{\phi^3}{\phi_c^3} \right] \quad (1)$$

Here ϕ_c is the critical phase difference at which the supercurrent I is at its maximum. Note that this critical phase is proportional to the ratio of the nanowire length L and the superconducting coherence length ξ as $\phi_c = L/(\xi\sqrt{3})$. Here I_c is the maximum possible current, which is achieved if $\phi = \phi_c$. It is called the critical current since at this current, superconductivity breaks down.

To simplify notations, we rewrite the CPR as

$$\frac{I(\phi)}{I_0} = \frac{\phi}{\phi_0} - \left[\frac{\phi}{\phi_0} \right]^3 \quad (2)$$

Here ϕ is the phase difference of the condensate wave function taken between the ends of the wire, I is the supercurrent in the wire, $\phi_0 = \sqrt{3}\phi_c$, and $I_0 = (3\sqrt{3}/2)I_c$. According to the approximate CPR given above, $I = 0$ if $\phi = \phi_0$. The maximum of this CPR occurs at $\phi/\phi_0 = 1/\sqrt{3}$ and the maximum supercurrent at that point is $2I_0/3\sqrt{3}$, so this value is the actual critical current if one measures just one nanowire.

Now, we introduce a perpendicular magnetic field bias B , which generates a phase gradient in the electrodes that is linear with B . Physically speaking, the magnetic field creates Meissner screening currents, which induce the phase gradients in the direction in which the vector potential is zero¹⁸. Now, let us say, the period of the superconducting quantum interference device (SQUID) formed by the two parallel wires is ΔB . Then the phase shift between the wires equals 2π when $B = \Delta B$. Let us introduce a normalized magnetic field $b = B/\Delta B$. If the phase difference on wire-1 is ϕ_1 , then the phase difference on wire-2 is $\phi_2 = \phi_1 + 2\pi b$. Now, define a global phase difference between the electrodes as $\phi = (\phi_1 + \phi_2)/2$, the total supercurrent of the device is:

$$\frac{I(\phi)}{I_0} = \frac{\phi_1}{\phi_0} - \left[\frac{\phi_1}{\phi_0} \right]^3 + \frac{\phi_2}{\phi_0} - \left[\frac{\phi_2}{\phi_0} \right]^3 \quad (3)$$

or

$$\frac{I(\phi)}{I_0} = \frac{2\phi}{\phi_0} - \frac{(\phi - \pi b)^3 + (\phi + \pi b)^3}{\phi_0^3} \quad (4)$$

Here, we assume that there are no trapped vortices between the wires or in the electrodes.

Expanding out the CPR obtains the following equation:

$$\frac{I(\phi)}{I_0} = \left(\frac{2(\phi_0^2 - 3(\pi b)^2)}{\phi_0^3} \right) \phi - \left(\frac{2}{\phi_0^3} \right) \phi^3 \quad (5)$$

It is imperative to note that applying a non-zero phase shift between the nanowires (see Eq. 5) suppresses the linear term in the CPR, but not the cubic term. This means that by

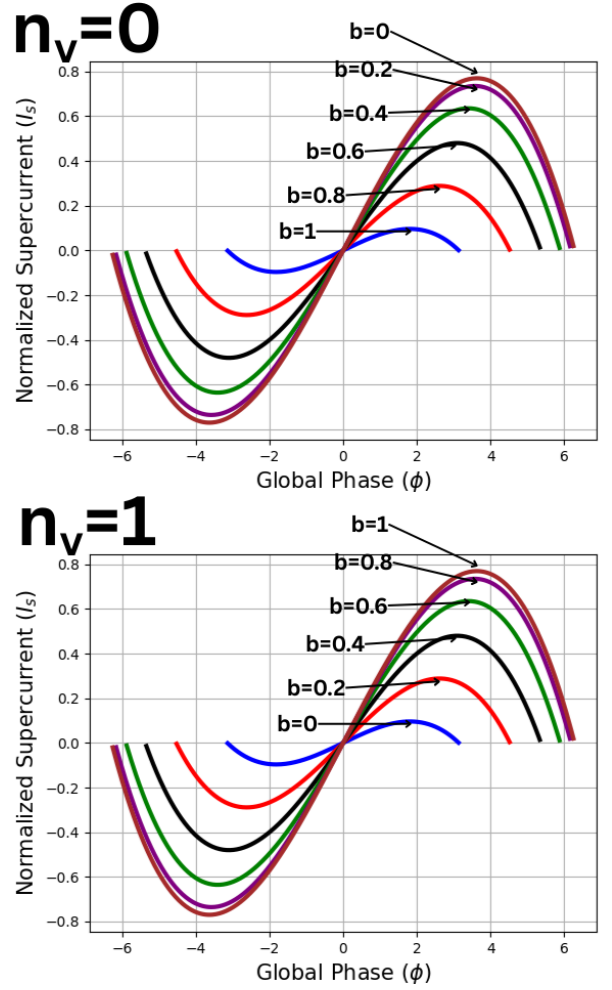


FIG. 2. Evolution of the total supercurrent versus magnetic field for $n_v = 0$ and $n_v = 1$. For sufficiently high values of $b - n_v$, the local maxima and minima are suppressed towards zero supercurrent.

increasing the phase shift between the wires, which equals $\phi_{shift} = 2\pi b$, one can make the cubic term more and more significant in comparison to the linear term. This is a key finding that provides a solution to making nanowire qubits.

Another interesting observation is that if the critical current of each wire is too large, one can make the critical current of the qubit smaller by increasing the phase shift ϕ_{shift} . Let us show this explicitly. Let us now write CPR in the form

$$I/I_0 = A\phi - D\phi^3 = A\phi \left(1 - \frac{D}{A}\phi^2 \right) \quad (6)$$

According to Eq. 5, the coefficients defining the quadratic and the quartic terms are:

$$A = A(b) = \frac{2(\phi_0^2 - 3\pi^2 b^2)}{\phi_0^3} \quad (7)$$

$$D = \frac{2}{\phi_0^3} \quad (8)$$

Then the location of the maximum of the current is defined by zero derivative, which occurs at $\phi^2 = \phi_{max}^2 = A/3D$. For example, in zero field the maximum is at $\phi^2 = \phi_0^2/3 = \phi_c^2$, as expected. Then the maximum current (i.e., the critical current) of the Dayem loop is $I_{max} = AI_0\phi_{max}(1 - (D/A)\phi_{max}^2) = (2/3)AI_0\sqrt{A/3D}$. Thus, the critical current is $I_{max} = (2/3\sqrt{3})I_0A^{3/2}D^{-1/2} = (2/3\sqrt{3}\sqrt{2})I_0(2/\phi_0 - 6\pi^2b^2/\phi_0^3)^{3/2}(\phi_0^3)^{1/2}$. From this one observes that the critical current of the SQUID goes to zero if the magnetic field satisfies $1 - 3\pi^2b^2/\phi_0^2 = 0$ or $b = \phi_0/\sqrt{3}\pi = \phi_c/\pi$, where ϕ_c is the critical phase of one nanowire, as introduced above. This makes sense since $\phi_{shift} = 2\pi b$, so if $b = \phi_c/\pi$ then the phase bias on each wire, at zero external bias current, equals its critical phase. Therefore, at the field $b = \phi_c/\pi$, the Meissner current in the wires equals their critical current.

The key property of the Dayem loop is that when $A(b)$ approaches zero, D remains constant. So the interference effect suppresses the critical current, but it does not suppress the nonlinearity. Such a result will be crucial to realizing a qubit with a sufficiently high anharmonicity.

It should be emphasized that if the current in each wire remains, at all times, a few percent lower than its critical current, then the phase slip rate is exponentially low if the temperature is near zero. Thus, the vorticity of the device remains unchanged with time, even as the magnetic field is tuned to make the CPR more nonlinear.

So far, we have assumed that there are no trapped vortices between the nanowires. Let us briefly consider what would happen if some number of vortices, n_v , is present in the loop formed by the two wires. Each vortex generates a total phase shift of 2π , so the total phase shift becomes $\phi_{shift} = 2\pi(b - n_v)$. (Note that each vortex in the SQUID loop contributes a phase bias of π per wire. It is assumed that the electrodes act macroscopically, so the phase bias on them is negligible if a few vortices are present in the SQUID loop.) So the CPR becomes:

$$\frac{I(\phi)}{I_0} = \left(\frac{2(\phi_0^2 - 3\pi^2(b - n_v)^2)}{\phi_0^3} \right) \phi - \left(\frac{2}{\phi_0^3} \right) \phi^3 \quad (9)$$

This equation (Eq. 9) would be a representation of the Little-Parks effect if n_v is allowed to adjust to minimize the quantity $|b - n_v|$. Yet, at near zero temperature, at which qubits normally operate, n_v cannot change because the phase slip rate is controlled by the Arrhenius activation exponent, which is extremely small at low temperatures. The protection against phase slips occurs because the phase slips in superconducting wires have normal cores, and it costs significant condensation energy to suppress superconductivity even in a small segment of a nanowire.

This dependence of the total supercurrent on the normalized magnetic field is illustrated in Fig. 2 for $n_v = 0$ and $n_v = 1$. We observe that the maximum of the CPR shifts to a lower current as the magnetic field is increased. We also observe that it is possible to shift the local maximum of the total current function, $I(\phi)$, close to zero if the vorticity is changed. This is an important characteristic since for transmon qubit applications,

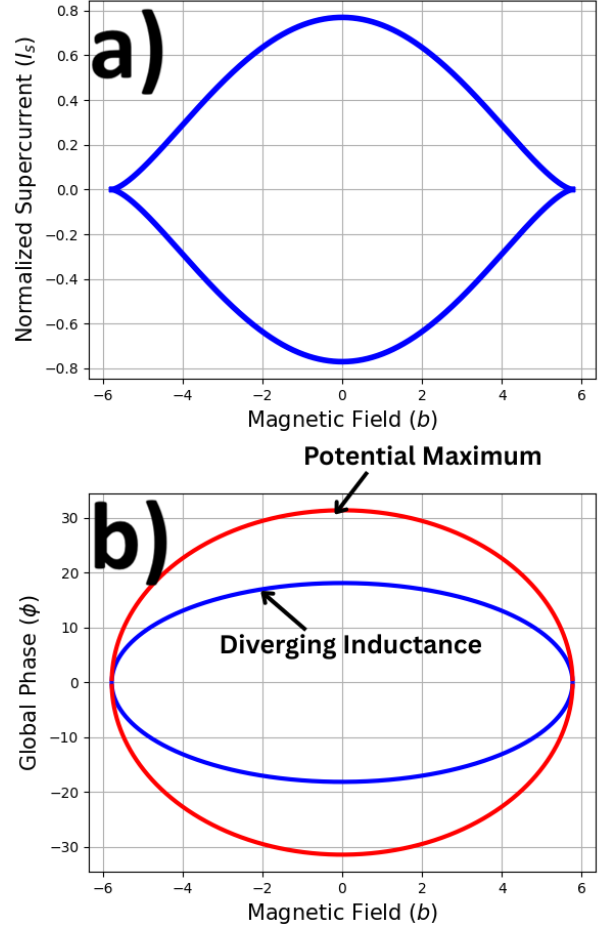


FIG. 3. (a) $I_c(b)$ curve for $\phi_0 = 10\pi$. (b) Plots of (ϕ, b) with $\phi_0 = 10\pi$, where the inductance diverges (blue), and the potential reaches its maximum (red). Note, they are not the same curve.

the critical current has to be larger but comparable to the current introduced by just one energy quantum in the resonator LC-circuit, which constitutes the qubit.

Also, according to Eq. 9, the critical current can be suppressed not only by changing the magnetic field but also by introducing vorticity into the loop. This can be achieved by driving the magnetic field to sufficiently high values. Since n_v does not change at low temperature, the possibility of having different vorticity values n_v constitutes a possibility to design programmable qubits if such a Dayem loop is used as the nonlinear inductive element of the qubit.

An example plot of the critical current versus magnetic field is shown in Fig. 3a. There we find that the critical current can be pushed all the way to zero if the magnetic field is increased, assuming that phase slips do not occur in the wire and the vorticity, n_v , does not change. That means that the nonlinear inductance regime can be pushed to as low a current as necessary with an external magnetic field. This is the key to achieving a transmon qubit functionality with a two-nanowire qubit, because in a transmon qubit, the current produced by just one microwave photon, absorbed by the qubit, has to be

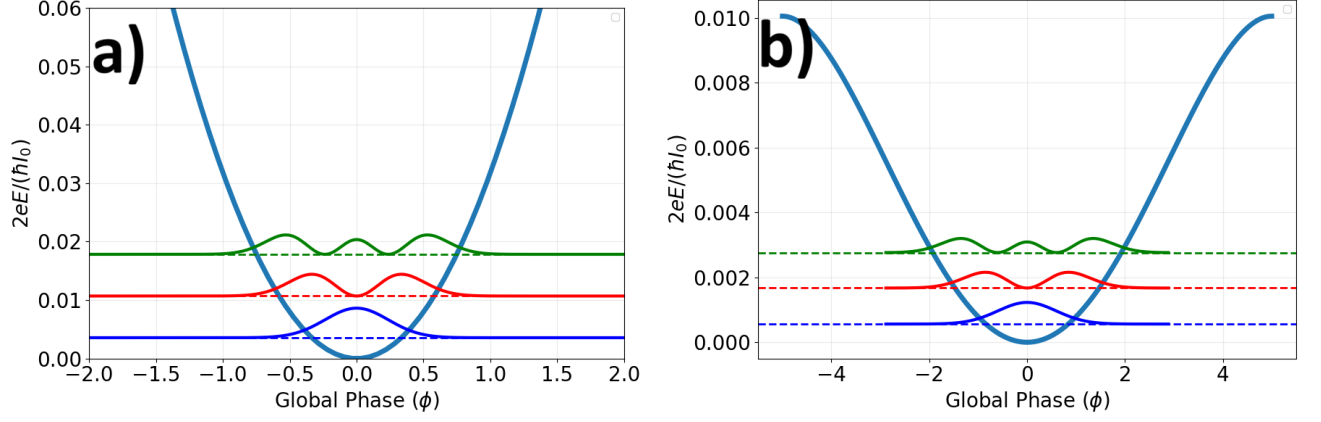


FIG. 4. **Increasing anharmonicity of a Dayem loop qubit with a cubic order CPR via magnetic-field tuning.** Shown is the potential energy together with the lowest three eigenstates: ground (blue), first excited (red), and second excited (green). Solid curves represent the eigenfunctions, while dashed horizontal lines indicate the corresponding eigenenergies. The vertical axis shows the normalized energy $2eE/(\hbar I_0)$, with $n_v = 0$, $I_0 = 1 \mu\text{A}$, corresponding to an energy normalization factor $\hbar I_0/2e = 497 \text{ GHz}$. The qubit parameters are $E_c/h \approx 0.3 \text{ GHz}$ and $\phi_0 = 10\pi$. The qubit excitation energy depends on the magnetic field. Note, all the presented energies below have units of $\hbar I_0/(2e)$. (a) *Zero magnetic field* ($b = 0$). The maximum of the potential is $U_{max} = 15.7$. The energy levels are E_0 , E_1 , and E_2 . The ground state is $E_0 = 3.566 \times 10^{-3}$. The qubit excitation energy is $E_{01} = E_1 - E_0 = 7.13 \times 10^{-3}$. Thus, the qubit excitation energy is $E_{01} = 3.54 \text{ GHz}$. The second excitation energy gap is $E_{12} = E_2 - E_1 = E_{01} + \alpha$, where $\alpha = -2.427 \times 10^{-6}$ is the absolute anharmonicity. This yields a small relative anharmonicity $\alpha_r = (E_{12} - E_{01})/E_{01} = -1 + (E_{01} + \alpha)/E_{01} = \alpha/E_{01} = -0.00034$, which is -0.034% . The small anharmonicity arises because the eigenfunctions are localized far below the potential maximum, where the potential is nearly harmonic, resulting in an almost linear energy spectrum. (b) *Finite magnetic field* ($b = 5.7$). The applied magnetic field pushes down the maximum of the potential, and the wave functions expand and become closer to the maximum. Thus, the effect of the non-linear terms of the potential is enhanced. The maximum of the potential energy is $U_{max} = 1 \times 10^{-2}$. The ground state energy is $E_0 = 5.6145 \times 10^{-4}$, the first excitation energy $E_{01} = E_1 - E_0 = 1.111 \times 10^{-3}$, and the second one is $E_{12} = E_2 - E_1 = 1.093 \times 10^{-3}$. Therefore, the absolute anharmonicity is $\alpha = E_{12} - E_{01} = -1.8 \times 10^{-5}$. This results in a significantly increased relative anharmonicity of $\alpha_r = (E_{12} - E_{01})/E_{01} = -0.016$ which is -1.6% .

enough to change the slope of the CPR by at least a few percent.

B. Increasing anharmonicity with magnetic field in a simple model of a Dayem loop qubit

To find the energy levels and the eigenstates of our proposed Dayem loop qubit, one needs to write its Hamiltonian. We need to choose its kinetic and potential energies, to build an analogy with a harmonic oscillator of slight anharmonicity. We will assume that the Coulomb charging energy of the device acts as its "kinetic energy" while the energy of the condensate in the nanowires, which is controlled by the phase difference ϕ , acts as its "potential energy". Let us first construct the quantum operator of the kinetic energy. Classically, the kinetic energy of an electrical system is given by the Coulomb energy $T = Q^2/(2C)$ where Q is the charge in the system and C is the capacitance between the electrodes (antennas) connected to the nanowires. This term is always quadratic in Q . Note that the charge is proportional to the time derivative of the phase ϕ , which is considered as the "coordinate" of the oscillator. This is because the voltage is $V = Q/C$ and the time derivative of the phase (coordinate) is $d\phi/dt = 2eV/\hbar = 2eQ/C\hbar$.

Similarly, the quantum mechanical "kinetic energy" operator for superconducting quantum circuits is $\hat{T} = \hat{Q}^2/(2C)$

where $\hat{Q} = 2e\hat{N}$. Here, \hat{N} is the number operator that returns the number of pairs of electrons in the superconductor condensate, in excess of the charge neutrality point. In the phase basis, the number operator can be rewritten as $\hat{N} = i\partial_\phi$. Therefore, defining the Coulomb charging energy for one electron as $E_c = e^2/(2C)$, the kinetic energy term is $-4E_c\partial_\phi^2$. Here e is the charge of one electron.

Moreover, the potential energy corresponding to any current-phase relationship (CPR) can be calculated as $U(\phi) = \hbar/(2e) \int_0^\phi I_s(\phi') d\phi'$. Integrating Eq. 9 one obtains the potential energy U as $U(\phi)$ as:

$$U(\phi) = \left(\frac{\hbar I_0}{2e}\right) \left(\frac{1}{2}A\phi^2 - \frac{1}{4}D\phi^4\right) \quad (10)$$

where A and D have been defined and discussed above. The maximum of this function occurs at $\phi = \sqrt{A/D}$ and the corresponding energy barrier is $U_{max} = \frac{\hbar I_0 A^2}{2e 4D} = \frac{\hbar I_0}{2e} (\phi_0/2) (1 - 3\pi^2 b^2/\phi_0^2)^2$.

The potential energy function represents an approximately harmonic oscillator with a slight anharmonicity given by the fourth power (quartic) term. As was mentioned before, the introduction of a non-zero phase shift between the nanowires suppresses the quadratic term coefficient $A = A(b) = 2/\phi_0 - 6\pi^2 b^2/\phi_0^3$ while keeping the quartic term constant with the magnetic field. Such a result is again emphasized to be im-

perative towards realizing a sufficiently high anharmonicity in nanowire-SQUID transmons.

The phase difference ϕ , also viewed as the "position" or "coordinate" of the oscillator, is described by the corresponding quantum mechanical operator $\hat{\phi}$.

The Hamiltonian is $\hat{H} = \hat{T} + \hat{U}$ is:

$$\hat{H} = -4E_c \partial_{\phi}^2 + \left(\frac{\hbar I_0}{2e} \right) \left(\frac{1}{2} A \phi^2 - \frac{1}{4} D \phi^4 \right) \quad (11)$$

For this slightly anharmonic Hamiltonian, we first find the qubit excitation frequency f_0 , in zeroth order in D . (Here and always, $D = 2/\phi_0^3 = 2/(3\sqrt{3}\phi_c^3)$, the coefficient in front of the quartic term, is assumed to be a small parameter.) The so-called plasma frequency of the qubit, ω , is controlled by the quadratic term as

$$\hbar\omega = 2\sqrt{\frac{E_c \hbar I_0 A}{e}} \quad (12)$$

(For comparison, note that for a traditional transmon qubit, this well-known formula would be $\omega = \sqrt{8E_c E_J}$, see Appendix A) Here, the parameter A is dependent on the interference effect between the two wires and thus it is a function of the magnetic field. Note that for practical applications, the transmon plasma frequency should be in the range between 1 and 10 GHz, meaning that ω is in the range between $6 \times 10^9 \text{ s}^{-1}$ and $6 \times 10^{10} \text{ s}^{-1}$. This is achieved by changing E_c and A . The Coulomb charging energy E_c is controlled by the geometry of the antennas, and A is controlled by the length of the nanowires as well as by the applied magnetic field. If the critical current of the wire is too large (since it is difficult to make homogeneous nanowires with a critical current below 100 nA, which is usually needed for transmons with convenient and usable parameters), the magnetic field can be used to reduce f_0 by reducing A .

The correspondence between E_J and the coefficient in front of the quadratic term is $E_J \leftrightarrow (\frac{\hbar I_0}{2e})A$. Thus, zero-point fluctuations are

$$\phi_{zpf}^4 = \frac{2E_c}{A} \frac{2e}{\hbar I_0} = \frac{4eE_c \phi_0^3}{\hbar I_0 (2\phi_0^2 - 6\pi^2 b^2)} \quad (13)$$

As is derived in the Appendix C, the anharmonicity is proportional to the product of zero point fluctuations to the power four and the coefficient in front of the quartic term. In other words, the anharmonicity of a transmon qubit is $\alpha = -12K_4 \phi_{zpf}^4$ where K_4 is the coefficient in front of the quartic term. In the considered case of the Dayem loop qubit, the coefficient K_4 is $K_4 = (\frac{\hbar I_0}{2e}) \frac{D}{4}$. Then, its anharmonicity is calculated to be:

$$\alpha = -12K_4 \phi_{zpf}^4 = -6 \frac{D}{A} E_c = -\frac{6E_c}{\phi_0^2 - 3\pi^2 b^2} \quad (14)$$

Note that if $b = 0$ then $\alpha = -6E_c/\phi_0^2$, where ϕ_0 is a critical phase at which the superfluid density in a wire is suppressed, and the supercurrent becomes zero.

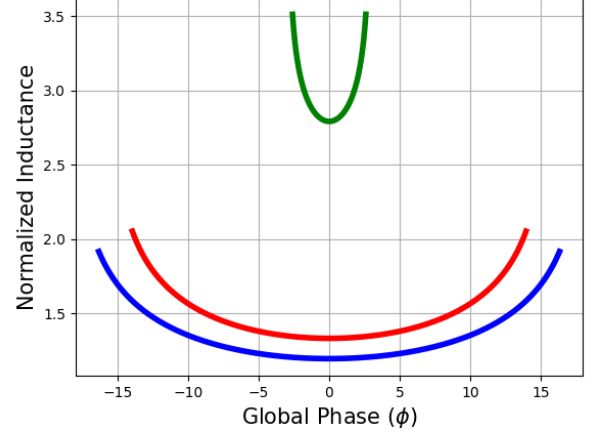


FIG. 5. **Plots of log (base 10) of normalized inductance of a symmetric 2 nanowire SQUID** Here, we consider a device with $\phi_0 = 10\pi$ at magnetic fields of $b = 0$ (blue), $b = 3$ (red), $b = 5.7$ (green).

We solve the Hamiltonian (Eq. 11) numerically using Python with boundary conditions $\psi(\pm\sqrt{\phi_0^2/3 - \pi^2 b^2}) = 0$. The physical meaning of the boundary conditions is that at the phase difference where the supercurrent goes to zero, we assume there is an infinite height potential wall. Later, we will verify that such a boundary condition has little to no effect on the wavefunctions because the wavefunctions are strongly localized at $\phi = 0$.

The resulting evolution of the potential landscape, together with its associated eigenvalues and eigenfunctions as a function of the applied magnetic field, is shown in Fig. 4. As the magnetic field increases, the eigenfunctions shift closer to the top of the potential well, enhancing the influence of the nonlinear components of the potential on the energy spectrum. This increased nonlinearity leads to a corresponding enhancement of the anharmonicity. The energy is normalized by the constant $\hbar I_0/(2e)$, where $I_0 = 3\sqrt{3}I_c/2$ and I_c denotes the critical current of each nanowire. We note that the metastable states remain localized near $\phi = 0$. Overall, these results demonstrate that the relative anharmonicity can be strongly enhanced by the application of a magnetic field.

To verify the accuracy of our numerically calculated metastable states, we utilize two techniques. First, we computed the energy levels using the Wentzel–Kramers–Brillouin (WKB) semiclassical approximation (Appendix D), finding good quantitative agreement with the numerical spectrum. Secondly, we also moved the infinite potential wells by about 10 percent, either closer to zero or away from zero. We observed a negligible change in the relative anharmonicity of about 1%. This result is because the wavefunctions are localized very close to the potential minimum, and approach zero probability exponentially as they approach the infinite potential energy wall. Therefore, the chosen boundary condition has no significant effect on the wavefunctions and the numerically calculated metastable states are accurate.

C. Inductance

To achieve a high anharmonicity, the kinetic inductance of the device has to have a sufficient nonlinearity. Here, we derive the conditions necessary for the inductance to diverge. The objective is to push the nonlinear inductance regime towards sufficiently low supercurrents, e.g., similar to the transmon's operating currents. The kinetic inductance L_k is computed as:

$$\begin{aligned} L_k &= \left(\frac{\Phi_0}{2\pi}\right) \left(\frac{dI}{d\phi}\right)^{-1} = \left(\frac{\Phi_0}{2\pi}\right) \frac{1}{I_0(A - 3D\phi^2)} \\ &= \left(\frac{\Phi_0}{2\pi}\right) \frac{\phi_0^3}{I_0(2\phi_0^2 - 3(\phi - \pi b)^2 - 3(\phi + \pi b)^2)} \end{aligned} \quad (15)$$

The evolution of the log (base 10) of the inductance curve (normalized by $\Phi_0/(2\pi)$) with respect to the applied magnetic field is shown in Fig. 5. From Eq. 15, it follows that the inductance diverges if:

$$\frac{\phi^2}{\phi_{\max}^2} + \frac{b^2}{b_{\max}^2} = 1 \quad (16)$$

Where $\phi_{\max} = \phi_0/\sqrt{3} = \phi_c$ and $b_{\max} = \phi_0/(\pi\sqrt{3})$. A plot of Eq. 16 is shown in Fig. 3b along with the curve corresponding to the maximum of the potential. Note that these curves do not align. The inductance divergence ellipses stays within the maximum potential ellipse. Thus, the device wave function might be able to sample the divergence region, which is the key factor allowing this nanowire-SQUID qubit to achieve higher anharmonicity compared to single-wire devices. Indeed, according to Eq. 16, increasing b will reduce, as low as necessary, the global phase at which the inductance diverges, as $\phi_{div} = \sqrt{\frac{A}{3D}} = \sqrt{\frac{\phi_0^2 - 3\pi^2 b^2}{3}} = \sqrt{\phi_c^2 - \pi^2 b^2}$. This means that even if a single wire has a low anharmonicity, the SQUID will have a higher anharmonicity if the magnetic field is tuned.

D. Anharmonicity

A high anharmonicity is necessary to reduce a many-level quantum system to an effective qubit. The absolute and relative anharmonicity is defined as:

$$\alpha = E_{12} - E_{01}, \quad \alpha_r = \alpha/E_{01} \quad (17)$$

Where, $E_{12} = E_2 - E_1$ and $E_{01} = E_1 - E_0$. Next, consider our weakly anharmonic Hamiltonian $\hat{H} = -4E_c \partial_\phi^2 + (\hbar I_0/(2e))(A\phi^2/2 - D\phi^4/4)$. The coefficients A and D are defined in Eq. 7 and Eq. 8. We can apply time-independent perturbation theory to approximate the eigenenergies up to first order. Keeping the energy level j arbitrary (j is a non-negative integer), we can obtain the following approximation (See Appendix E for more details):

$$\begin{aligned} E_m &\approx 2\sqrt{\frac{2E_c \hbar I_0 (\phi_0^2 - 3\pi^2 [b - n_v]^2)}{\phi_0^3 e}} \left(j + \frac{1}{2}\right) \\ &\quad - \frac{2E_c}{\phi_0^2 - 3\pi^2 [b - n_v]^2} (6j^2 + 6j + 3) \end{aligned} \quad (18)$$

The resulting expressions for the absolute and relative anharmonicity are:

$$\alpha = -\frac{6E_c}{\phi_0^2 - 3\pi^2 [b - n_v]^2} \quad (19)$$

$$\alpha_r = -\frac{3\phi_0^{3/2}}{2(\phi_0^2 - 3\pi^2 [b - n_v]^2)^{3/2}} \sqrt{\frac{2eE_c}{\hbar I_0}} \quad (20)$$

Here, as always, n_v is the number of fluxons trapped between the two nanowires. This result demonstrates that applying a phase shift, with either an applied magnetic field or by introducing vortices between the two nanowires, will increase anharmonicity. In particular, as the total phase shift between the wires increases, the absolute anharmonicity increases and the plasma frequency decreases. Both of these effects, therefore, increase the relative anharmonicity of the device.

Such an effect is qualitatively different than the single nanowire qubit, where the anharmonicity is only dominated by the length of the nanowire and its critical current. We also observe that the excitation energy ($E_{01} = E_1 - E_0$) is proportional to $\sqrt{I_0 A}$, therefore, if E_{01} is too large due to the critical current of the nanowires being too high, one can always reduce it by applying an appropriate magnetic field, since A is reduced with magnetic field.

IV. REALISTIC NANOWIRE CPR MODELS

A. Zero-temperature current-phase relationship (CPR) of superconducting nanowires

In the previous sections, we studied a simplified model in which the nonlinear correction to the nanowire current-phase relationship (CPR) takes a cubic form. This approximation is valid at temperatures near the critical temperature or, potentially, for extremely short nanowires. However, transmon qubits operate near absolute zero temperature, where the CPR can deviate significantly from this cubic form. A more realistic zero-temperature model is therefore required to obtain reliable estimates of the proposed qubit performance.

Microscopic calculations based on the Usadel equations²⁶ have previously been carried out by Ref.²⁰. We digitize their reported CPR curves and find that they can be modeled with high accuracy using a simple power-law form, as described below.

While Eq. 2 accurately captures the CPR at high operating temperatures, the low-temperature CPR curves reported in Ref.²⁰ show a qualitatively different behavior. In particular, the CPR becomes increasingly linear at low phase bias as

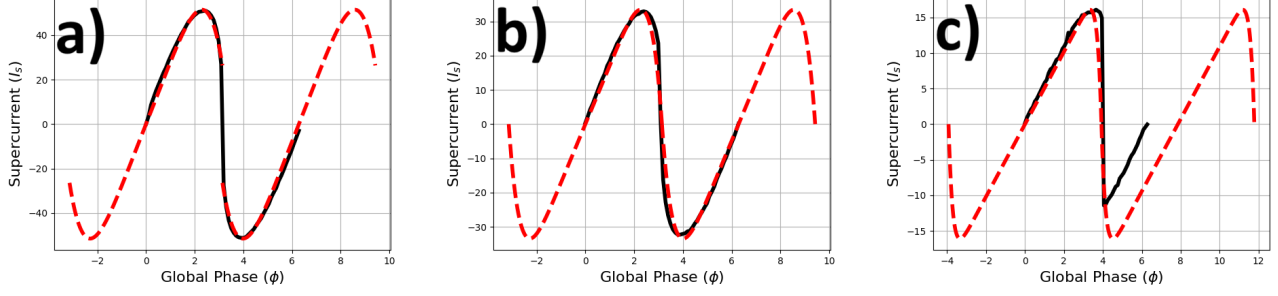


FIG. 6. **Power-law fits to zero-temperature nanowire current–phase relationships.** Black curves show current–phase relationships calculated from the Usadel equations in Ref.²⁰ at $T = 0.15\text{K}$ with a nanowire width of 45nm . Red curves show fits to the generalized power-law model of Eq. 21. Across a wide range of parameters and CPR shapes, the model reproduces the numerically calculated curves with high accuracy, capturing both the extended linear regime at small phase bias and the sharp onset of nonlinearity near the critical current. (a) Here, the length of the nanowire is 15nm . The corresponding power law fit had the following parameters: $m = 2$, $a = 0.7$, $\phi_0 = 2\pi$, $I_0 = 44$. (b) Here, the length of the nanowire is 45nm . The corresponding power law fit had the following parameters: $m = 3$, $a = 1$, $\phi_0 = 2\pi$, $I_0 = 27$. (c) Here, the length of the nanowire is 240nm . The corresponding power law fit had the following parameters: $m = 9$, $a = 1$, $\phi_0 = 2.5\pi$, $I_0 = 10$. These results justify the use of the generalized $(2m + 1)$ power-law CPR in the perturbative analysis that follows.

the temperature is reduced, leading to the onset of nonlinearity shifting closer to the critical current. To account for these deviations, we introduce a generalized power-law model that fits both the results of Ref.²³ and those of Ref.²⁰:

$$\frac{I(\phi)}{I_0} = \frac{\phi}{\phi_0} - a \left(\frac{\phi}{\phi_0} \right)^{2m+1} \quad (21)$$

Here, a is a dimensionless constant which defines the strength of the nonlinearity, and m is a positive integer.

This CPR gives zero current ($I = 0$) if $\phi = \phi_{zero} = \phi_0 a^{-1/2m}$. And the maximum of the current occurs at $\phi = \phi_{max} = \phi_0 / (a(2m + 1))^{1/2m}$. It is interesting to calculate the difference:

$$\phi_{zero} - \phi_{max} = \phi_0 a^{-1/(2m)} \left[a^{1/m} - (2m + 1)^{-1/(2m)} \right] \quad (22)$$

An interesting observation is that as wires get longer and m gets larger, this difference approaches zero, although it is always a positive number. Thus, for longer wires, we get the expected result that the maximum of the CPR occurs close to the point where the supercurrent drops to zero.

For example, if $m = 2$ then $\phi_{zero} = \phi_0 a^{-1/4}$. Also, if $a = 1$ then $I = 0$ at $\phi_{zero} = \phi_0$ at any m . Also, for $m = 2$, $\phi_{max} = \phi_0 / (5a)^{1/4}$, which is less than ϕ_{zero} as expected.

A practical justification for the power-law CPR given above is obtained by directly comparing it to the CPR curves calculated using the microscopic theory and reported in Ref.²⁰. We find an excellent agreement, as is demonstrated in Fig. 6.

If the non-linear term is absent, then the CPR is exactly linear, and it is impossible to make a qubit. Such a case has been analyzed previously in relation to memory elements²⁵. But qubits are possible for any $m > 0$, such as the Likharev CPR discussed above, $m = 1$, since the nonlinear correction is cubic. Two features of this model are noted. In general, the nonlinear correction is presented as $2m + 1$, to emphasize that the CPR remains an odd function of ϕ . Second, as m increases,

the CPR nonlinearity shifts closer to the critical phase. The cubic CPR is recovered as the special case $a = 1$ and $m = 1$, or, as will be discussed below, if two wires are connected in parallel, forming a SQUID.

B. Restoration of the cubic term in CPR due to quantum interference between two nanowires

We now extend our power-law CPR model to the Dayem loop qubit by introducing a phase shift $\pi(b - n_v)$ between the wires, analogous to the treatment used for the cubic CPR. Here, b denotes the applied perpendicular magnetic field (normalized), and n_v is the integer number of vortices trapped between the nanowires. The total supercurrent of the device is then:

$$\frac{I(\phi)}{I_0} = \frac{2\phi}{\phi_0} - a \frac{(\phi - \pi[b - n_v])^{2m+1} + (\phi + \pi[b - n_v])^{2m+1}}{\phi_0^{2m+1}} \quad (23)$$

In what follows, we will assume $n_v = 0$. Our main finding is that even if $m > 1$, we can still get a desirable cubic nonlinearity if two wires are connected in parallel and a magnetic field is amplified between them. The magnetic field creates a phase shift $\phi_{shift} = 2\pi b$. The cubic term of the SQUID CPR occurs as follows. For one wire, the CPR is $i_1 = \delta_1 - a\delta_1^{2m+1}$, where we use the normalized current $i_1 = I_1/I_0$ and the normalized phase difference on the wire, $\delta_1 = \phi_1/\phi_0$. The expression for wire 2 is the same except that $\delta_2 = \phi_2/\phi_0 = (\phi_1 + \phi_{shift})/\phi_0 = \delta_1 + \delta_{shift}$. And a is a constant defining the amplitude of the nonlinear term. The global normalized phase difference is $\delta = (\delta_1 + \delta_2)/2$. With these notations, the SQUID normalized CPR is:

$$i = (\delta - \delta_{shift}/2) + (\delta + \delta_{shift}/2) - a(\delta - \delta_{shift}/2)^{2m+1} - a(\delta + \delta_{shift}/2)^{2m+1} \quad (24)$$

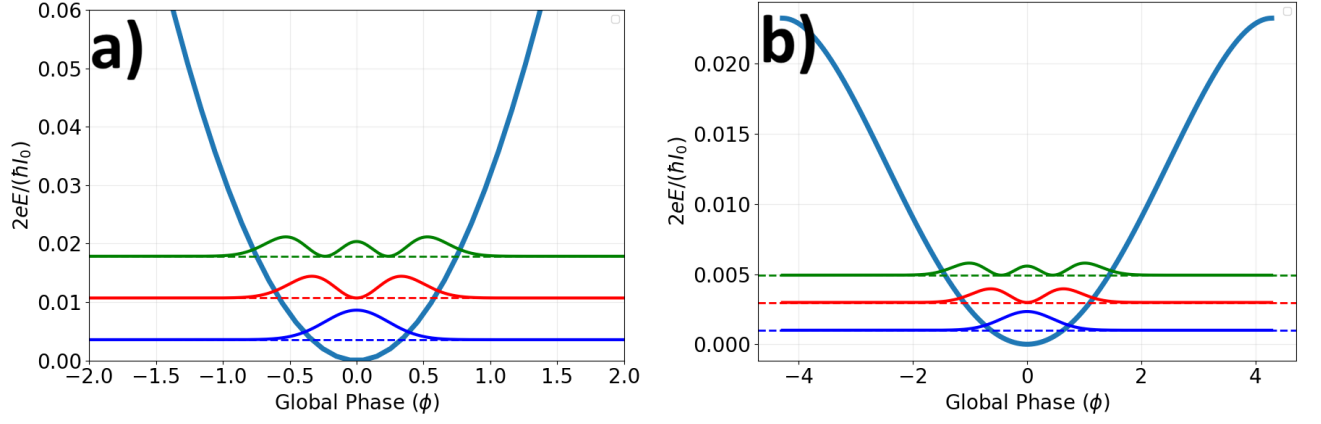


FIG. 7. **Wave functions and anharmonicity of a Dayem loop qubit with a fifth-order CPR. Magnetic-field effect.** Shown is the potential energy together with the lowest three eigenstates: ground (blue), first excited (red), and second excited (green). Solid curves represent the eigenfunctions, while dashed horizontal lines indicate the corresponding eigenenergies. The vertical axis shows the normalized energy $2eE/(\hbar I_0)$, with $n_v = 0$, $I_0 = 1 \mu\text{A}$, corresponding to an energy normalization factor $\hbar I_0/2e = 497 \text{ GHz}$. The qubit parameters are $E_c/h \approx 0.3 \text{ GHz}$ and $\phi_0 = 10\pi$. The qubit excitation energy depends on the magnetic field. Note, all the presented energies below have units of $\hbar I_0/(2e)$. Here, $a = 1$. (a) *Zero magnetic field* ($b = 0$). In the perturbative picture, at $b = 0$, the potential reduces to a simple harmonic oscillator with zero anharmonicity. The energies are therefore $\hbar\omega(j+1/2)$ where j is an integer and $\hbar\omega = 4\sqrt{\hbar I_0 E_c/(2e\phi_0)} = 3.6196 \times 10^{-24}$, corresponding to $\omega/2\pi = 5.5\text{GHz}$. (b) *Finite magnetic field* ($b = 6.55$). Similar to the cubic CPR case, the magnetic field pushes the wavefunctions closer to the maximum of the potential, thereby increasing the impact of the non-linearity. The maximum of the potential energy is $U_{max} = 2.32 \times 10^{-2}$. The ground state energy is $E_0 = 9.989 \times 10^{-4}$, the first excitation energy $E_{01} = E_1 - E_0 = 1.981 \times 10^{-3}$, and the second one is $E_{12} = E_2 - E_1 = 1.945 \times 10^{-3}$. Therefore, the absolute anharmonicity is $\alpha = E_{12} - E_{01} = -3.6 \times 10^{-5}$. This results in a significantly increased relative anharmonicity of $\alpha_r = (E_{12} - E_{01})/E_{01} = -0.018$ which is -1.8% .

The first, linear, term of the expression is

$$i_{linear}(\delta) \approx \left[2 - 2a(2m+1) \left(\frac{\delta_{shift}}{2} \right)^{2m} \right] \delta$$

Apparently, this term can be reduced by the phase shift $\delta_{shift} = \phi_{shift}/\phi_0 = 2\pi b/\phi_0$. In fact, it can be reduced to any low value, even to zero. In general, the linear term controls the frequency of the qubit. Thus, the conclusion is that the frequency can be controlled in a wide range. Here, it is assumed that the vorticity is zero and that there are no phase slips (which change the vorticity) during the qubit operation. This assumption is reasonable since to create a phase slip in a nanowire, one needs to create a normal region, which costs the condensation energy, which is usually quite large for a homogeneous nanowire.

The cubic correction term of the general CPR is

$$i_{cubic}(\delta) = -2a \binom{2m+1}{3} \left(\frac{\delta_{shift}}{2} \right)^{2m-2} \delta^3$$

It is linear at zero magnetic field, but it increases in magnitude if a magnetic field is applied, which generates the phase shift δ_{shift} . Thus, the calculations done in the previous sections, based on the cubic CPR, are relevant in general since the cubic term can be restored due to quantum interference between the two nanowires.

In the following sections, we perform a perturbative analysis of a few examples and compute the resulting relative anharmonicity for (i) the fifth-order CPR ($m = 2$), (ii) the seventh-order CPR ($m = 3$), and (iii) the general case of arbitrary m .

We demonstrate that even nanowires with highly linear CPRs can support appreciable anharmonicity, provided that a sufficient phase shift is induced between the two wires. This establishes a practical route toward building qubits from otherwise weakly nonlinear nanowire elements.

C. CPR with fifth order nonlinearity

In this section, we analyze the total supercurrent and the resulting anharmonicity for a symmetric SQUID with a fifth-order ($m = 2$) current-phase relationship (CPR). The total current is

$$\frac{I(\phi)}{I_0} = \frac{2\phi}{\phi_0} - a \frac{(\phi - \pi[b - n_v])^5 + (\phi + \pi[b - n_v])^5}{\phi_0^5} \quad (25)$$

To simplify the discussion, we assume $n_v = 0$. Then

$$\frac{I(\phi)}{I_0} = \left(\frac{2}{\phi_0} - \frac{10a\pi^4 b^4}{\phi_0^5} \right) \phi - \frac{20a\pi^2 b^2}{\phi_0^5} \phi^3 - \frac{2a}{\phi_0^5} \phi^5 \quad (26)$$

Interestingly, a term cubic in ϕ appears in the current, due to quantum interference between the wires. It is clear that the linear term is now controlled by the magnetic field b and can be made as small as necessary to achieve the right qubit frequency. The cubic term actually gets larger in magnitude if the magnetic field is increased. The fifth power term does not depend on the magnetic field. The linear term goes to zero if

$$b = \pm \frac{\phi_0}{\pi(5a)^{1/4}} \quad (27)$$

This corresponds exactly to the condition that the Meissner current in the electrodes induces a phase shift on each nanowire such that the current in each nanowire equals its maximum possible supercurrent.

We restrict our analysis to highly localized wavefunctions, $|\phi| \ll \phi_c$, and expand the CPR in powers of ϕ up to third order. This approximation yields an effective quartic potential of the form

$$U(\phi) \approx \frac{\hbar I_0}{2e} \left[\frac{\phi_0^4 - 5a(\pi[b - n_v])^4}{\phi_0^5} \phi^2 - \frac{5a(\pi[b - n_v])^2}{\phi_0^5} \phi^4 \right] \quad (28)$$

Two key features emerge from this expression. First, the phase difference between the nanowires, $\pi(b - n_v)$, suppresses the quadratic term through the factor $\phi_0^4 - 5a(\pi[b - n_v])^4$. Second, and in contrast to the cubic CPR case ($m = 1$), the quartic term is explicitly increasing by the phase shift, scaling as $(b - n_v)^2$. By increasing $(b - n_v)^2$, one simultaneously decreases the harmonic term and enhances the nonlinear correction, thereby amplifying the overall nonlinearity of the device. One can compare this to the case when the CPR of each wire is cubic. In that case, the quartic term is independent of the applied phase difference. In the case considered here, when the CPR of each wire has a fifth-power nonlinearity, the phase shift directly strengthens the nonlinear component of the potential.

The anharmonicity can be obtained using first-order time-independent perturbation theory. Matching the coefficients of the effective potential to the standard quartic oscillator form given in Appendix E yields a closed-form approximation for the relative anharmonicity as a function of magnetic field:

$$\alpha_r = -\sqrt{\frac{2eE_c}{\hbar I_0}} \frac{15a(\pi[b - n_v])^2 \phi_0^{5/2}}{(\phi_0^4 - 5a(\pi[b - n_v])^4)^{3/2}} \quad (29)$$

This expression further emphasizes the importance of the phase shift between nanowires. In particular, when $(b - n_v) = 0$, then in the perturbative picture, the quartic contribution vanishes and the relative anharmonicity becomes zero. Therefore, a finite phase shift (finite b) is always necessary to achieve a nonzero anharmonicity in the fifth-order CPR.

Let us consider an example $a = 1$, $n_v = 0$, $\phi_0 = 10\pi$, $E_c/h \approx 0.3$ GHz, and $I_0 = 1 \mu\text{A}$. In this case, the quadratic term goes to zero at $b = (\phi_0/\pi)/(5a)^{1/4} = 6.68$. The qubit excitation energy depends on the magnetic field (see below). Such an example is shown in Fig. 7. There, all the presented energies are normalized by $\hbar I_0/(2e) = 497$ GHz, and plotted on the graphs are the potential energy together with the lowest three eigenstates: ground (blue), first excited (red), and second excited (green). Solid curves represent the eigenfunctions, while dashed horizontal lines indicate the corresponding eigenenergies. The vertical axis shows the normalized energy $2eE/(\hbar I_0)$.

The qubit excitation energy depends on the magnetic field. The case of zero magnetic field ($b = 0$) is shown in Fig. 7a. According to the Appendix C, the frequency of such a qubit is $\omega^2 = 4K_1K_2$, where $K_1 = 4E_c/\hbar^2$ and $K_2 = \frac{\hbar I_0}{2e}(1/\phi_0 - 5a(\pi b)^4/\phi_0^5)$. So $\omega^2 = \frac{8E_c I_0}{e\hbar}(1/\phi_0 - 5a(\pi b)^4/\phi_0^5)$. Neglecting all terms beyond the cubic term in the CPR, and

for $b = 0$, the potential reduces to that of a simple harmonic oscillator, implying vanishing anharmonicity ($\alpha_r = 0$) in this approximation. The quantized energy levels are therefore approximately $\hbar\omega(j + 1/2)$ where j is an integer and $\hbar\omega = 4\sqrt{\hbar I_0 E_c/(2e\phi_0)} = 5.776 \times 10^{-24}\text{J}$, corresponding to the qubit excitation frequency of 8.7 GHz and zero anharmonicity ($\alpha_r = 0$) within this approximation.

Next, if higher order corrections are taken into account, then the anharmonicity is (see the Appendix C(6)): $\alpha = -180K_6\phi_{zpf}^6 = -180K_6(E_c/K_2)^{3/2}$. Let us calculate first zero point fluctuations of the phase for $b = 0$ (see the Appendix C):

$$\phi_{zpf}^4 = \frac{\hbar^2 K_1}{4 K_2} = \phi_0 \frac{2eE_c}{\hbar I_0} \quad (30)$$

Substituting the numbers chosen above, one gets $\phi_{zpf} = 0.2367$. Thus, the size of the wave function is much smaller than the critical phase, as it should be for the perturbation model to work well. Next, we evaluate the coefficient K_6 by integrating Eq. 26 for $b = 0$. Thus $K_6 = \frac{a}{3\phi_0^5} \frac{\hbar I_0}{2e} = 1.089 \times 10^{-8} \times 497\text{GHz}$. With this we obtain the anharmonicity $\alpha = -180 \times (0.2367)^6 \times 1.089 \times 10^{-8} \times 497\text{GHz} = 171\text{Hz}$, which is very small. The relative anharmonicity in this case is $\alpha_r = 171\text{Hz}/E_{01} = 171\text{Hz}/(\hbar\omega) = 171\text{Hz}/8.7\text{GHz} = -1.97 \times 10^{-8}$, which is only 0.00000197%. This is too small for any practical qubit application.

A numerical Hamiltonian solver was employed to compute the relative anharmonicity. However, due to grid discretization effects, the solver is unable to reliably resolve extremely small anharmonicities. In particular, when $a = 0$, the Hamiltonian reduces to that of a quantum harmonic oscillator, for which the relative anharmonicity is exactly $\alpha_r = 0$. Nevertheless, the numerical solver yields a finite value, denoted $\alpha_{r,a=0}$, which is about an order of magnitude larger than the perturbative estimate of 10^{-8} obtained in the previous paragraph. Consequently, the relative anharmonicity computed for $a = 1$, denoted $\alpha_{r,a=1}$, is found to be of the same order as $\alpha_{r,a=0}$, indicating that it is dominated by numerical error. Although $\alpha_{r,a=0}$ can be reduced to approximately 10^{-7} by refining the discretization, $\alpha_{r,a=1}$ remains of comparable magnitude. This value therefore serves as an upper bound for $\alpha_{r,a=1}$. So it is concluded that in the case $b = 0$ the numerical error dominates the computed result. In general, both the perturbative and numerical approaches consistently indicate that, at zero magnetic field, the relative anharmonicity is extremely small for the chosen set of parameters. Yet, as is discussed below, an appropriately chosen magnetic field can mitigate this problem and increase the anharmonicity to about 1%, which is good enough for practical applications of the Dayem loop qubit.

An example numerical calculation result for a finite magnetic field ($b = 6.55$) is given in Fig. 7b. Similar to the cubic CPR case, the magnetic field pushes the maximum of the potential to the localization region of the wavefunction, thereby increasing the impact of the non-linearity. For the parameters given above, the normalization constant is as before $\hbar I_0/(2e) = 497$ GHz. The maximum of the potential energy is $U_{max} = 2.32 \times 10^{-2}(\hbar I_0/(2e)) = 11.5\text{GHz}$. The ground state energy is $E_0 = 9.989 \times 10^{-4}(\hbar I_0/(2e))$, the first

excitation energy $E_{01} = E_1 - E_0 = 1.981 \times 10^{-3} (\hbar I_0 / (2e)) = 0.985 \text{GHz}$, and the second one is $E_{12} = E_2 - E_1 = 1.945 \times 10^{-3} (\hbar I_0 / (2e)) = 0.967 \text{GHz}$. Therefore, the absolute anharmonicity is $\alpha = E_{12} - E_{01} = -3.6 \times 10^{-5} (\hbar I_0 / (2e)) = 0.018 \text{GHz}$. This results in a practically acceptable relative anharmonicity of $\alpha_r = (E_{12} - E_{01}) / E_{01} = -0.018$ which is -1.8% .

Another method is as follows. The relative anharmonicity, if a cubic term is present in the CPR and thus a quartic term is present in the potential energy, is $\alpha = -12K_4 \phi_{zpf}^4$. The quartic factor is $K_4 = \frac{\hbar I_0}{2e} \frac{5a\pi^2 b^2}{\phi_0^3} = 6.9 \times 10^{-5} \times 497 \text{GHz} = 34.4 \text{MHz}$. Now, the zero point fluctuations is given by $\phi_{zpf}^4 = (\hbar^2/4)(K_1/K_2) = (0.44559)^4$, the absolute anharmonicity can be calculated as $K_4 \times -12 \times (0.44559)^4 = -3.27 \times 10^{-6} \times 497 \text{GHz} = -16.8 \text{MHz}$. Thus, the relative anharmonicity is $-16.8 \text{MHz} / 967 \text{MHz} = -0.017$ or -1.7% , with good agreement with numerical simulations.

Yet one more evaluation method is given by Eq. 29. If we put the parameters chosen above in Eq. 29, we get a relative anharmonicity of -0.016 , which is -1.6% . Again, we observe good agreement with numerical results.

More generally, this provides the first concrete illustration of a broader trend: although, at low temperatures, in longer nanowires $m > 1$ and so the nanowire CPRs are highly nonlinear only very near the critical current, the introduction of a non-zero phase difference between the wires can drive the nonlinearity to lower currents by inducing a cubic nonlinearity. Also, the phase shift between the wires reduces the qubit frequency by reducing the total critical current. Since a phase shift can be induced by a small external magnetic field (typically a few Gauss), such an effect enables homogeneous nanowire qubits, without requiring any interfaces like in gate-mons for example, or any external current bias.

D. Seventh Order CPR

In this section, we extend our perturbative analysis on the symmetric SQUID towards nanowires exhibiting a seventh-order ($m = 3$) current-phase relationship (CPR). The total current is

$$\frac{I(\phi)}{I_0} = \frac{2\phi}{\phi_0} - a \frac{(\phi - \pi[b - n_v])^7 + (\phi + \pi[b - n_v])^7}{\phi_0^7} \quad (31)$$

Similar to the fifth-order CPR section, we will restrict our analysis to highly localized wavefunctions, and expand this supercurrent out to cubic order in ϕ . Integrating this CPR yields a quartic potential function:

$$U(\phi) \approx \frac{\hbar I_0}{2e} \left[\frac{\phi_0^6 - 7a(\pi[b - n_v])^6}{\phi_0^7} \phi^2 - \frac{35a(\pi[b - n_v])^4}{2\phi_0^7} \phi^4 \right] \quad (32)$$

The structure of the potential energy for the seventh-order CPR parallels that of the fifth-order case, with a stronger dependence on the phase difference between the two nanowires.

Suppose, for example, that there are no trapped vortices in the loop ($n_v = 0$). Then, as the magnetic field increases, the quadratic term in the potential is suppressed through the factor $\phi_0^6 - 7a(\pi b)^6$, while the quartic term is increased proportionally to b^4 . Such a result reflects the fact that even if the power of the nonlinearity in the CPR is 7, it is still possible to gain a cubic nonlinearity in the CPR and, correspondingly, a quartic nonlinearity in the potential energy.

Physically, this behavior implies that nanowires whose CPRs are approximately linear at low currents can still be driven into a strongly anharmonic regime by introducing a sufficiently large phase imbalance between the two nanowires. The higher power of $(\pi[b - n_v])$ appearing in the quartic term indicates that the onset of nonlinearity is more sensitive to magnetic fields in higher-order CPRs than in lower-order ones. As a result, devices governed by a seventh-order CPR require larger phase shifts to achieve appreciable anharmonicity.

Note, the maximum magnetic field that the device can support is equivalent to the magnetic field for which the quadratic term is exactly zero. Therefore, $b_{\max} = \phi_0 / (\pi(7a)^{1/6})$. In the below examples, $\phi_0 = 10\pi$ and $a = 1$, therefore $b_{\max} \approx 7.23$.

Using Appendix E, we can calculate the relative anharmonicity of the device as:

$$\alpha_r = -\sqrt{\frac{2eE_c}{\hbar I_0}} \frac{105a(\pi[b - n_v])^4 \phi_0^{7/2}}{2(\phi_0^6 - 7a(\pi[b - n_v])^6)^{3/2}} \quad (33)$$

As an example, we will calculate the relative anharmonicity with the parameters $E_c/h \approx 0.3 \text{GHz}$, $\phi_0 = 10\pi$, $I_0 = 1 \times 10^{-6}$. At $b = 0$, in the perturbative picture, the anharmonicity is zero since the potential function reduces to a simple harmonic oscillator with energies $\hbar\omega(j + 1/2)$ j is an integer and $\hbar\omega = \sqrt{\hbar I_0 E_c / (2e\phi_0)} = 3.6196 \times 10^{-24} \text{J}$, corresponding to $\omega/2\pi = 5.5 \text{GHz}$.

Next, we apply $b = 7$ (which is less than $b_{\max} \approx 7.23$) to the system and assume $n_v = 0$ (no trapped vortices). Then the ground state energy is $E_0 = 1.4912 \times 10^{-3} \frac{\hbar I_0}{2e}$, and the first excitation energy is $E_{01} = E_1 - E_0 = 2.9682 \times 10^{-3} \frac{\hbar I_0}{2e}$. The second excitation energy is $E_{12} = E_2 - E_1 = 2.938 \times 10^{-3} \frac{\hbar I_0}{2e}$. Therefore, the absolute anharmonicity is $\alpha = E_{12} - E_{01} = -3.02 \times 10^{-5} \frac{\hbar I_0}{2e}$. Then, the relative anharmonicity is $\alpha_r = \alpha / E_{01} = -0.011$ or -1.1% , which is sufficiently strong for transmon operations.

We note that, in contrast to the fifth-order CPR relative anharmonicity, a larger magnetic field was necessary to push the anharmonicity up to one percent. Such an effect is reflected in the fact that in the seventh-order CPR, the nonlinear regime is shifted closer to the critical current. Thus, a larger phase difference is required to drive the system to its nonlinear regime. Moreover, we continue to observe a general trend that nanowires with higher order nonlinearities in the CPRs can be used as nonlinear inductors for qubits, provided that the phase difference between the wires is made sufficient by the magnetic field.

E. General Case

In this section, we generalize our perturbative analysis towards symmetric SQUIDs with nanowires, demonstrating a current phase relationship on the order of $2m + 1$, where m is treated as an arbitrary integer. The total supercurrent of the device is:

$$\frac{I(\phi)}{I_0} = \frac{2\phi}{\phi_0} - a \frac{(\phi - \pi[b - n_v])^{2m+1} + (\phi + \pi[b - n_v])^{2m+1}}{\phi_0^{2m+1}} \quad (34)$$

To fully expand Eq. 34, we employ the binomial theorem to expand the polynomials $(\phi \pm \pi[b - n_v])^{2m+1}$. Firstly, integrating this term to yield the potential energy, then collecting terms up to the quartic order, corresponds to the following:

$$U(\phi) = \frac{\hbar I_0}{2e} \left[\frac{\phi_0^{2m} - a(2m+1)(\pi[b - n_v])^{2m}}{\phi_0^{2m+1}} \phi^2 - \frac{a(4m^2 - 1)(m)(\pi[b - n_v])^{2(m-1)}}{6\phi_0^{2m+1}} \phi^4 \right] \quad (35)$$

Here, this potential function emphasizes a general trend observed in highly linear CPRs with $m > 1$. In general:

Increasing $|b - n_v|$: quadratic term \downarrow quartic term \uparrow

Such a result has the effect of driving the system towards the non-linear regime as the magnetic field increases, and so the phase bias between the two nanowires increases. Moreover, the effect of the phase bias is increased as the CPRs approach a highly linear behavior for small ϕ . This reflects the fact that as m increases, the non-linear regime is pushed towards currents near the critical current. Therefore, a larger phase bias is required to push the total system relative anharmonicity towards a few percent. Then, using Appendix E, we arrive at the formula for the relative anharmonicity of an $2m + 1$ -th order CPR.

$$\alpha_r = -\sqrt{\frac{2eE_c}{\hbar I_0} \frac{a(2m+1)(m)(2m-1)(\pi[b - n_v])^{2(m-1)}\phi_0^{m+1/2}}{2(\phi_0^{2m} - a(2m+1)(\pi[b - n_v])^{2m})^{3/2}}} \quad (36)$$

The general expressions derived above unify the behavior observed in the cubic, fifth, and seventh order CPRs. As the order m increases, the CPR becomes increasingly linear near $\phi = 0$, while the nonlinear corrections are pushed closer to the critical current. However, the presence of a phase difference between the two nanowires can overcome this linearity by simultaneously suppressing the quadratic term and amplifying the quartic term in the effective potential.

In general, a larger ϕ_0 decreases the relative anharmonicity of the entire system. Therefore, shorter nanowires are favorable towards building qubits.

In general, increasing the magnetic field enhances the anharmonicity for all $m > 1$, with the sensitivity to the phase shift growing rapidly with CPR order. Importantly, these results demonstrate that even nanowires with highly linear zero-temperature CPRs can function as qubits by simply applying a phase shift between the wires' magnetic design alone.

V. CONCLUSION

We proposed a qubit design involving two parallel superconducting nanowires, which can be called "Dayem loop qubit" since it does not contain tunnel junctions or any interfaces between different materials. For a nanowire with a current phase relationship (CPR) of cubic non-linearity, we find closed curves representing the inductance divergence points, which appear elliptical in the phase difference - magnetic field plane. We then applied perturbation theory to approximate the anharmonicity. We present evidence that for longer wires, the current-phase relationship (CPR) has a power-law deviation from the linear behavior, in which the power becomes larger as the wire is made longer. This fact makes it more difficult to make qubits with longer nanowires. Yet, we demonstrate that this problem can be mitigated if two nanowires form a superconducting quantum interference device (SQUID). In this case, the interference between the wires leads to an increased nonlinearity by generating a cubic term in the current-phase relationship (CPR) of the device. This is true even if the nonlinearity of the CPR of each wire taken separately is of a higher than cubic order. In this case, we used first-order perturbation theory to approximate the anharmonicity of such nanowires. Then, we found that even though superconducting nanowires by themselves might have a low level of nonlinearity, which is apparent only very near the critical current, the interference effect between the two nanowires leads to a cubic nonlinearity restoration in the CPR of the entire device, thus enabling qubit operations.

Appendix A: Analogy Between a Generic Anharmonic Oscillator and Superconducting Qubits

In this appendix, we establish the analogy between a generic weakly anharmonic oscillator and the superconducting transmon qubit. We then extend the same framework to the Dayem Loop transmon qubit with a non-sinusoidal current-phase relation (CPR).

1. Generic Anharmonic Oscillator

We consider a one-dimensional oscillator with Hamiltonian

$$H = \frac{\hat{p}^2}{2m_1} + \frac{1}{2}m_1\omega^2x^2 + U_{\text{anh}}(x) \iff K_1\hat{p}^2 + K_2x^2 - K_4x^4 \quad (A1)$$

where m_1 is the mass of the particle and $U_{\text{anh}}(x) = -K_4x^4$ is a weak nonlinear correction to the harmonic potential. The

generic coefficients are defined as $K_1 = 1/(2m_1)$ and $K_2 = m_1\omega^2/2$. The harmonic part defines the zero-point fluctuation amplitude

$$x_{\text{zpf}}^4 = \frac{\hbar^2 K_1}{4 K_2} = \left(\frac{\hbar}{2m_1\omega} \right)^2 \quad (\text{A2})$$

The anharmonicity of the spectrum is

$$\alpha = (E_2 - E_1) - (E_1 - E_0) = E_2 - 2E_1 + E_0 \quad (\text{A3})$$

To first order in perturbation theory,

$$\alpha = \langle 2|U_{\text{anh}}(\hat{x})|2\rangle - 2\langle 1|U_{\text{anh}}(\hat{x})|1\rangle + \langle 0|U_{\text{anh}}(\hat{x})|0\rangle \quad (\text{A4})$$

For a purely quartic perturbation $U_{\text{anh}}(x) = -K_4x^4$, this evaluates to

$$\alpha = -12K_4x_{\text{zpf}}^4 = -3\hbar^2 \frac{K_1 K_4}{K_2} \quad (\text{A5})$$

Thus the anharmonicity scales with the fourth power of the zero-point fluctuations.

2. Transmon Qubit as a Weakly Anharmonic Oscillator

The transmon Hamiltonian is

$$H_{\text{tr}} = 4E_c N^2 - E_J \cos \phi \quad (\text{A6})$$

where ϕ is the superconducting phase difference and N is the Cooper-pair number operator with

$$[\phi, N] = i, \quad N = -i \frac{\partial}{\partial \phi} \quad (\text{A7})$$

In the transmon regime $E_J \gg E_c$, the Josephson potential can be expanded as

$$-E_J \cos \phi \approx -E_J + \frac{1}{2}E_J\phi^2 - \frac{E_J}{24}\phi^4 + \dots \quad (\text{A8})$$

Identifying

$$x \leftrightarrow \phi \quad p \leftrightarrow \hbar N \quad m_1 \leftrightarrow \hbar^2/(8E_c)$$

the Hamiltonian maps onto Eq. (A1) with

$$K_1 = \frac{4E_c}{\hbar^2} \quad K_2 = \frac{E_J}{2} \quad K_4 = \frac{E_J}{24}$$

The quadratic term defines a harmonic oscillator with frequency

$$\omega = \frac{\sqrt{8E_c E_J}}{\hbar} \quad (\text{A9})$$

and phase zero-point fluctuations

$$\phi_{\text{zpf}}^4 = \frac{2E_c}{E_J} \quad (\text{A10})$$

Using Eq. (A5), the transmon anharmonicity becomes

$$\alpha_{\text{tr}} = -12 \left(\frac{E_J}{24} \right) \phi_{\text{zpf}}^4 = -E_c \quad (\text{A11})$$

which is the standard first-order result.

3. Dayem Loop Qubit

For a Dayem Loop qubit with a CPR of cubic order, the Hamiltonian can be written as

$$\hat{H} = -4E_c \partial_\phi^2 + \left(\frac{\hbar I_0}{2e} \right) \left(\frac{1}{2} A \phi^2 - \frac{1}{4} D \phi^4 \right) \quad (\text{A12})$$

The coefficients are

$$A(b) = \frac{2}{\phi_0} - \frac{6\pi^2 b^2}{\phi_0^3} \quad D = \frac{2}{\phi_0^3} = \frac{2}{3\sqrt{3}\phi_c^3} \quad (\text{A13})$$

Matching to Eq. (A1) gives

$$K_1 = \frac{4E_c}{\hbar^2} \quad K_2 = \frac{\hbar I_0}{2e} \left(\frac{1}{\phi_0} - \frac{3\pi^2 b^2}{\phi_0^3} \right) \quad K_4 = \frac{\hbar I_0}{2e} \frac{1}{2\phi_0^3}$$

The zero-point phase fluctuations are therefore

$$\phi_{\text{zpf}}^4 = \frac{\hbar^2 K_1}{4 K_2} = \frac{E_c}{(\hbar I_0/2e)} \frac{\phi_0}{1 - 3\pi^2 b^2/\phi_0^2} \quad (\text{A14})$$

Using Eq. (A5), the anharmonicity becomes

$$\alpha = -12K_4\phi_{\text{zpf}}^4 = -\frac{6E_c}{\phi_0^2 - 3\pi^2 b^2} \quad (\text{A15})$$

Appendix B: Current–Phase Relationship of a Superconducting Nanowire from Ginzburg–Landau Theory

In this appendix, we derive the current–phase relationship (CPR) of a uniform superconducting nanowire using one-dimensional Ginzburg–Landau (GL) theory. The derivation is valid near the superconducting critical temperature T_c , where GL theory applies, and assumes a homogeneous wire carrying a uniform supercurrent, neglecting phase-slip processes.

1. Ginzburg–Landau Free Energy

We consider a superconducting wire oriented along the x -direction. The GL free-energy density is

$$f = \alpha |\psi|^2 + \frac{\beta}{2} |\psi|^4 + \frac{\hbar^2}{2m^*} \left| \left(\partial_x - i \frac{2e}{\hbar} A_x \right) \psi \right|^2 \quad (\text{B1})$$

where $\psi(x)$ is the superconducting order parameter, m^* is the effective mass for superconducting electrons, and A_x is the vector potential.

We write the order parameter in amplitude–phase form,

$$\psi(x) = |\psi| e^{i\theta(x)} \quad (\text{B2})$$

and define the gauge-invariant phase gradient

$$q \equiv \partial_x \theta - \frac{2e}{\hbar} A_x \quad (\text{B3})$$

Assuming a uniform wire with constant current, both $|\psi|$ and q are spatially uniform.

2. Condensate Suppression by Superflow

With the assumptions above, the gradient term in Eq. B1 reduces to

$$\frac{\hbar^2}{2m^*} |\psi|^2 q^2 \quad (\text{B4})$$

Minimizing the free-energy density with respect to $|\psi|$ yields

$$\alpha + \beta |\psi|^2 + \frac{\hbar^2}{2m^*} q^2 = 0 \quad (\text{B5})$$

Defining the equilibrium condensate density

$$|\psi_0|^2 \equiv -\frac{\alpha}{\beta} \quad (\text{B6})$$

and the GL coherence length

$$\xi^2 \equiv \frac{\hbar^2}{2m^*|\alpha|} \quad (\text{B7})$$

Eq. B5 gives

$$|\psi|^2 = |\psi_0|^2 (1 - \xi^2 q^2) \quad (\text{B8})$$

This expression shows explicitly that the superconducting condensate is depleted by superflow.

3. Supercurrent Density

The supercurrent density in one dimension is

$$j_s = \frac{2e\hbar}{m^*} |\psi|^2 q \quad (\text{B9})$$

Substituting Eq. B8 into Eq. B9, we obtain

$$j_s(q) = \frac{2e\hbar}{m^*} |\psi_0|^2 q (1 - \xi^2 q^2) \quad (\text{B10})$$

This is the GL depairing-current relation: the current increases linearly with q at small phase gradients and is suppressed at large q due to suppression of the condensate density (suppression of superconductivity by the current).

4. Current–Phase Relationship

For a wire of length L , the total gauge-invariant phase difference across the wire is

$$\phi = \int_0^L q dx = qL \quad (\text{B11})$$

Thus,

$$q = \frac{\phi}{L} \quad (\text{B12})$$

Let S be the cross-sectional area of the wire. The total supercurrent is $I = S j_s$, which yields

$$I(\phi) = \frac{2e\hbar S}{m^*} |\psi_0|^2 \left(\frac{\phi}{L}\right) \left(1 - \xi^2 \frac{\phi^2}{L^2}\right) \quad (\text{B13})$$

Introducing the characteristic phase scale

$$\phi_0 \equiv \frac{L}{\xi} \quad (\text{B14})$$

The CPR can be written in compact form as

$$I(\phi) = I_0 \left(\frac{\phi}{\phi_0}\right) \left[1 - \left(\frac{\phi}{\phi_0}\right)^2\right] \quad (\text{B15})$$

where

$$I_0 \equiv \frac{2e\hbar S}{m^* \xi} |\psi_0|^2 \quad (\text{B16})$$

Equation B15 is the GL current–phase relationship of a superconducting nanowire. It is odd in ϕ , approximately linear at small phase differences, and exhibits a maximum corresponding to the depairing critical current. Note that the relative contribution of the quartic term is inversely proportional to ϕ_0^2 , i.e., it is inversely proportional to the squared length of the wire L . Thus, longer wires will generate a low value of the qubit anharmonicity. In the main part of the paper, we discuss how a larger anharmonicity can be achieved by making a SQUID with two nanowires.

5. Critical Current

The maximum of Eq. B10 occurs at

$$q\xi = \frac{1}{\sqrt{3}} \quad (\text{B17})$$

which corresponds to a phase difference

$$\phi_c = \frac{\phi_0}{\sqrt{3}} \quad (\text{B18})$$

The resulting depairing critical current is

$$I_c = \frac{4e\hbar S}{3\sqrt{3} m^* \xi} |\psi_0|^2 = \frac{2}{3\sqrt{3}} I_0 \quad (\text{B19})$$

This CPR differs qualitatively from the sinusoidal Josephson-junction CPR and reflects the distributed nature of superflow and condensate depletion in superconducting nanowires.

Appendix C: Anharmonicity from Zero-Point Fluctuations

In this appendix, we derive the absolute and relative anharmonicity using a zero-point fluctuation formulation. We will also compare the results with Appendix A.

1. Model Hamiltonian

We consider a one-dimensional quantum oscillator whose potential energy deviates weakly from harmonicity due to a quartic term. The Hamiltonian is given by

$$\hat{H} = \frac{\hat{p}^2}{2m_1} + \frac{1}{2}m_1\omega^2\hat{x}^2 - K_4\hat{x}^4 \quad (\text{C1})$$

where $\hat{x} = x$ is the coordinate operator which equals the coordinate itself, m_1 is the mass of the oscillator, ω is the harmonic frequency, and $K_4 > 0$ a softening anharmonicity parameter. The quartic (fourth power) term is assumed to be sufficiently small such that perturbation theory applies to the low-lying eigenstates.

2. Zero-Point Fluctuations

The natural length scale of the problem is set by the ground-state fluctuations of the harmonic oscillator. Introducing ladder operators, the position operator can be written as

$$\hat{x} = x_{\text{zpf}}(\hat{a} + \hat{a}^\dagger) \quad (\text{C2})$$

where the zero-point fluctuation amplitude is

$$x_{\text{zpf}} = \sqrt{\frac{\hbar}{2m_1\omega}} \quad (\text{C3})$$

Physically, x_{zpf} characterizes the spatial extent of the ground-state wavefunction and therefore determines how strongly the oscillator samples nonlinear terms in the potential.

Suppose we write the Hamiltonian in a more generic form as

$$\hat{H} = K_1\hat{p}^2 + K_2x^2 - K_4x^4 \quad (\text{C4})$$

where $K_1 = 1/2m_1$ and $K_2 = m_1\omega^2/2$. With this generic notation, the frequency of classical oscillations is

$$\omega^2 = 4K_1K_2 \quad (\text{C5})$$

and zero point fluctuation is

$$x_{\text{zpf}}^4 = \frac{\hbar^2 K_1}{4 K_2} \quad (\text{C6})$$

3. Dimensionless Anharmonicity Parameter

Substituting Eq. C2 into the quartic term of Eq. C1, the nonlinear contribution to the Hamiltonian becomes

$$-K_4\hat{x}^4 = -K_4x_{\text{zpf}}^4(\hat{a} + \hat{a}^\dagger)^4 = -\hbar\omega\lambda(\hat{a} + \hat{a}^\dagger)^4 \quad (\text{C7})$$

where we have introduced the dimensionless anharmonicity parameter

$$\lambda \equiv \frac{K_4x_{\text{zpf}}^4}{\hbar\omega} \quad (\text{C8})$$

This expression makes explicit that anharmonic effects scale with the fourth power of the zero-point fluctuations. Consequently, even a modest quartic coefficient K can lead to appreciable anharmonicity if x_{zpf} is large.

4. Energy Spectrum to First Order in λ

Treating the quartic term as a perturbation, the energy of the j th eigenstate is (j is a nonnegative integer)

$$E_j = \hbar\omega\left(j + \frac{1}{2}\right) - \hbar\omega\lambda(6j^2 + 6j + 3) \quad (\text{C9})$$

valid to first order in λ .

The three lowest energy levels are therefore

$$E_0 = \frac{1}{2}\hbar\omega - 3\hbar\omega\lambda = \frac{1}{2}\hbar\omega - 3K_4x_{\text{zpf}}^4 \quad (\text{C10})$$

$$E_1 = \frac{3}{2}\hbar\omega - 15\hbar\omega\lambda = \frac{3}{2}\hbar\omega - 15K_4x_{\text{zpf}}^4 \quad (\text{C11})$$

$$E_2 = \frac{5}{2}\hbar\omega - 39\hbar\omega\lambda = \frac{5}{2}\hbar\omega - 39K_4x_{\text{zpf}}^4 \quad (\text{C12})$$

The normalized energy levels are defined as $\varepsilon = E/\hbar\omega$. These levels are

$$\varepsilon_0 = \frac{1}{2} - 3\lambda \quad (\text{C13})$$

$$\varepsilon_1 = \frac{3}{2} - 15\lambda \quad (\text{C14})$$

$$\varepsilon_2 = \frac{5}{2} - 39\lambda \quad (\text{C15})$$

5. Anharmonicity

The anharmonicity is defined as the deviation from equal level spacing,

$$\alpha \equiv (E_2 - E_1) - (E_1 - E_0) = E_2 - 2E_1 + E_0 \quad (\text{C16})$$

The relative anharmonicity is defined as:

$$\alpha_r = \frac{\alpha}{E_1 - E_0} = \frac{E_2 - 2E_1 + E_0}{E_1 - E_0} = \frac{\varepsilon_2 - 2\varepsilon_1 + \varepsilon_0}{\varepsilon_1 - \varepsilon_0} \quad (\text{C17})$$

Substituting Eqs. C10–C15 into Eq. C16, the harmonic contributions cancel identically, yielding

$$\alpha = -12\hbar\omega\lambda \quad (\text{C18})$$

Using the definition of λ in Eq. C8, the anharmonicity can be expressed directly in terms of physical parameters as

$$\alpha = -12K_4x_{\text{zpf}}^4 \quad (\text{C19})$$

If λ is small then $E_1 - E_0 \approx \hbar\omega$. Then the relative anharmonicity is $\alpha_r = -12\lambda = -12\frac{K_4x_{\text{zpf}}^4}{\hbar\omega} = -6\frac{K_4x_{\text{zpf}}^4}{\hbar\sqrt{K_1K_2}} = -\frac{3\hbar\sqrt{K_1K_4}}{2K_2\sqrt{K_2}}$. Comparing this result to that of Appendix E, letting $4E_c/\hbar^2 = K_1$, $\beta_1 = K_2$, and $\gamma = -K_4$, we arrive at the same result obtained in Appendix E, thereby validating the zero-point fluctuations formulation.

6. Anharmonicity from Power-Law Potential

More generally, consider

$$\hat{H} = \frac{\hat{p}^2}{2m_1} + \frac{1}{2}m_1\omega^2\hat{x}^2 + U_{\text{anh}}(\hat{x}) \quad U_{\text{anh}}(x) = -K_n x^n \quad (\text{C20})$$

with K_n small. Introducing the dimensionless coordinate operator \hat{q} via

$$\hat{x} = x_{\text{zpf}} \hat{q} \quad (\text{C21})$$

The anharmonicity to first order becomes

$$\alpha = -K_n x_{\text{zpf}}^n \left(\langle 2|\hat{q}^n|2\rangle - 2\langle 1|\hat{q}^n|1\rangle + \langle 0|\hat{q}^n|0\rangle \right) \quad (\text{C22})$$

Because harmonic-oscillator probability densities are even functions of position, all diagonal moments of odd powers vanish. Consequently, for odd n ,

$$\alpha = 0 \quad (\text{odd } n, \text{ to first order in } K_n) \quad (\text{C23})$$

For even integer powers $n = 2(m+1)$ with the integer $m \geq 1$, the matrix-element combination in Eq. C22 evaluates to a universal numerical factor, yielding

$$\alpha = -K_n x_{\text{zpf}}^{2m+2} \frac{(2m+2)!}{2^m(m-1)!} \quad m \geq 1 \quad (\text{C24})$$

Equivalently, expressed directly in terms of n ,

$$\alpha = -K_n x_{\text{zpf}}^n \frac{n!}{2^{n/2-1} \left(\frac{n}{2} - 2\right)!} \quad n \text{ even}, n \geq 4 \quad (\text{C25})$$

For example, if the anharmonic term is quartic, then $n = 4$ and $\alpha = -12K_4 x_{\text{zpf}}^4$. This is an important result for the nanowire-SQUID qubit analysis since, in a nonzero magnetic field, we always find some nonzero quartic term in the potential energy. Higher-order terms might be relevant if the magnetic field is zero. Thus, if $n = 6$ then $\alpha = -180K_6 x_{\text{zpf}}^6 = -180K_6 (E_C/K_2)^{3/2}$, and if $n = 8$ then $\alpha = -2520K_8 x_{\text{zpf}}^8$, etc.

Appendix D: WKB Semi-Classical Approximation

This appendix section will be a summary of the application of the WKB semi-classical approximation towards estimating the energy levels of the Hamiltonian Eq. 11. The WKB (Wentzel-Kramers-Brillouin) semi-classical approximation is a technique for finding approximate solutions to quantum-mechanical problems when the potential energy varies slowly compared to the particle's wavelength. In other words, the total energy should be larger than the potential energy. In this paper, we used this technique to estimate the eigenenergies of the ground, first excited, and second excited states.

Using the Hamiltonian from Eq 11, the corresponding time-independent Schrödinger equation (SE) is:

$$[-4E_c \partial_\phi^2 + V(\phi)] \Psi(\phi) = E \Psi(\phi) \quad (\text{D1})$$

Here, the potential of the function is the following:

$$V(\phi) = \frac{\hbar I_0}{2e} \left(\left[\frac{\phi_0^2 - 3\pi^2 b^2}{\phi_0^3} \right] \phi^2 - \left[\frac{1}{2\phi_0^3} \right] \phi^4 \right) \quad (\text{D2})$$

Next, the WKB approximation uses the wavefunction ansatz of the form

$$\Psi(\phi) = \exp(iS(\phi)) \quad (\text{D3})$$

Where $S(\phi)$ is proportional to the action. Letting $S(\phi) = S_0 + S_1 + S_2 + \dots$ and inserting the wavefunction ansatz into Eq. D1, we obtain that $S(\phi)$ (up to first order):

$$S_0(\phi) = \pm \int_{\phi_1}^{\phi_2} \sqrt{\frac{E - V(\phi)}{4E_c}} \quad (\text{D4})$$

To obtain bound states, we impose the Bohr-Sommerfeld quantization condition:

$$\int_{\phi_1}^{\phi_2} \sqrt{\frac{E - V(\phi)}{4E_c}} = \left(j + \frac{1}{2} \right) \pi \quad (\text{D5})$$

Where $V(\phi_1) = V(\phi_2) = E$ are defined as the points where the wavefunction hits the potential energy function. Using Eq. D5, our code numerically estimates the total energy E . Below is a table of numerically calculated eigenenergies at various magnetic fields, compared with the WKB-approximated eigenenergies. Here, we use $\phi_0 = 10\pi$, $I_0 = 10^{-6}$, and $E_c/h \approx 0.3\text{GHz}$.

b	Numerical			WKB		
	E_0	E_1	E_2	E_0	E_1	E_2
0	0.00357	0.01070	0.01783	0.00357	0.01070	0.01784
1	0.00351	0.01054	0.01756	0.00351	0.01054	0.01757
2	0.00335	0.01004	0.01673	0.00335	0.01004	0.01673
3	0.00305	0.00914	0.01524	0.00305	0.00914	0.01524
4	0.00257	0.00772	0.01286	0.00257	0.00772	0.01286
5	0.00178	0.00535	0.00891	0.00178	0.00535	0.00891
5.5	0.00108	0.00325	0.00540	0.00108	0.00325	0.00541
5.7	0.00056	0.00167	0.00277	0.00056	0.00167	0.00276

TABLE I. Comparison of numerically computed and WKB eigenenergies for varying magnetic field b .

Based on the above table, the WKB calculated eigenenergies align with the numerically calculated eigenenergies. Therefore, we conclude that, based on this test, the numerically calculated eigenenergies are accurate.

Appendix E: Perturbation Theory for Generalized Quartic Potential

We briefly review the perturbation theory employed when approximating the absolute and relative anharmonicity for a

general quartic potential. Such a Hamiltonian can be written as:

$$\hat{H} = -4E_c \frac{\partial^2}{\partial \phi^2} + \beta_1 \phi^2 + \gamma \phi^4 \quad (\text{E1})$$

Next, we define the basic ladder operators for this system:

$$a = \frac{1}{2} \left(\frac{\beta_1}{E_c} \right)^{1/4} \phi + \left(\frac{E_c}{\beta_1} \right)^{1/4} \partial_\phi \quad (\text{E2})$$

$$a^\dagger = \frac{1}{2} \left(\frac{\beta_1}{E_c} \right)^{1/4} \phi - \left(\frac{E_c}{\beta_1} \right)^{1/4} \partial_\phi \quad (\text{E3})$$

Where $[a, a^\dagger] = 1$. Then, the complete Hamiltonian can be written in terms of the ladder operators:

$$\hat{H} = 4\sqrt{\beta_1 E_c} \left(a^\dagger a + \frac{1}{2} \right) + \frac{E_c \gamma}{\beta_1} (a^\dagger + a)^4 \quad (\text{E4})$$

Using perturbation theory, the leading order correction to the energy states can be computed as:

$$\frac{E_c \gamma}{\beta_1} \langle j | (a^\dagger + a)^4 | j \rangle = \frac{E_c \gamma}{\beta_1} (6j^2 + 6j + 3) \quad (\text{E5})$$

Therefore, the total energy can be computed as

$$E_m = 4\sqrt{\beta_1 E_c} \left(j + \frac{1}{2} \right) + \frac{E_c \gamma}{\beta_1} (6j^2 + 6j + 3) \quad (\text{E6})$$

We can then compute the anharmonicities:

$$\alpha = \frac{12\gamma E_c}{\beta_1}, \quad \alpha_r \approx \frac{3\gamma\sqrt{E_c}}{\beta_1^{3/2}} \quad (\text{E7})$$

Here, we assumed that $E_1 - E_0 \approx \hbar\omega$ for weak nonlinearity.

REFERENCES

- ¹Peter Shor, "Polynomial-time algorithms for prime factorization and discrete logarithms on a quantum computer," *SIAM Journal on Computing* **26**, 1484–1509 (1997).
- ²L. K. Grover, "Quantum mechanics helps in searching for a needle in a haystack," *Phys. Rev. Lett.* **79**, 325–328 (1997).
- ³Y. Nakamura, Y. A. Pashkin, and J. S. Tsai, "Coherent control of macroscopic quantum states in a single-Cooper-pair box," *Nature* **398**, 786–788 (1999).
- ⁴G. Q. AI and collaborators, "Quantum error correction below the surface code threshold," *Nature* **638**, 920–926 (2024).
- ⁵Leonid Glazman and Gianluigi Catelani, "Bogoliubov quasiparticles in superconducting qubits," *SciPost Phys. Lect. Notes* **31**, 1–40 (2021).
- ⁶Alexander Anferov, Kan-Heng Lee, Fang Zhao, Jonathan Simon, and David Schuster, "Improved coherence in optically defined niobium trilayer-junction qubits," *Phys. Rev. Appl.* **21**, 024047 (2024).
- ⁷D. Wang, Y. Wu, N. Pieczulewski, P. Garg, M. C. C. Pace, C. G. L. Böttcher, B. Mazumder, D. A. Muller, and H. X. Tang, "All-nitride superconducting qubits based on atomic layer deposition," *Nature Materials* (2026).
- ⁸C. Purmessur, K. Chow, B. Van Heck, and A. Kou, "Operation of a high-frequency, phase-slip qubit," *Nature Communications* **16**, 11456 (2025).
- ⁹J. E. Mooij and Y. V. Nazarov, "Superconducting nanowires as quantum phase-slip junctions," *Nature Physics* **2**, 169–172 (2006).
- ¹⁰C. G. L. Böttcher, E. Önder, T. Connolly, J. Zhao, C. Kvande, D. Q. Wang, P. D. Kurilovich, S. Vaitiekėnas, L. I. Glazman, H. X. Tang, and M. H. Devoret, "A transmon qubit realized by exploiting the superconductor-insulator transition," (2025), arXiv:2510.19983.
- ¹¹J. Ku, V. Manucharyan, and A. Bezryadin, "Superconducting nanowires as nonlinear inductive elements for qubits," *Phys. Rev. B* **82**, 134518 (2010).
- ¹²Jaseung Ku, Zack Yoscovits, Alex Levchenko, James Eckstein, and Alexey Bezryadin, "Decoherence and radiation-free relaxation in meissner transmon qubit coupled to abrikosov vortices," *Phys. Rev. B* **94**, 165128 (2016).
- ¹³R. Vijay, D. H. Slichter, and I. Siddiqi, "Observation of quantum jumps in a superconducting artificial atom," *Phys. Rev. Lett.* **106**, 110502 (2011).
- ¹⁴R. Vijay, E. M. Levenson-Falk, D. H. Slichter, and I. Siddiqi, "Approaching ideal weak link behavior with three dimensional aluminum nanobridges," *Applied Physics Letters* **96**, 223112 (2010).
- ¹⁵F. Faramarzi, P. Day, J. Glasby, S. Sypkens, M. Colangelo, R. Chamberlin, M. Mirhosseini, K. Schmidt, K. K. Berggren, and P. Mäuskopf, "Initial design of a W-Band Superconducting Kinetic Inductance QUBIT," *IEEE Transactions on Applied Superconductivity* **31**, 1–5 (2021).
- ¹⁶R. W. Simmonds, K. M. Lang, D. A. Hite, S. Nam, D. P. Pappas, and J. M. Martinis, "Decoherence in josephson phase qubits from junction resonators," *Phys. Rev. Lett.* **93**, 077003 (2004).
- ¹⁷Alexey Bezryadin, Chun Ning Lau, and Michael Tinkham, "Quantum suppression of superconductivity in ultrathin nanowires," *Nature* **404**, 971–974 (2000).
- ¹⁸D. S. Hopkins, D. Pekker, P. M. Goldbart, and A. Bezryadin, "Quantum interference device made by DNA templating of superconducting nanowires," *Science* **308**, 1762–1765 (2005).
- ¹⁹M. W. Brenner, S. Gopalakrishnan, J. Ku, T. J. McArdle, J. N. Eckstein, N. Shah, P. M. Goldbart, and A. Bezryadin, "Cratered lorentzian response of driven microwave superconducting nanowire-bridged resonators: Oscillatory and magnetic-field induced stochastic states," *Phys. Rev. B* **83**, 184503 (2011).
- ²⁰R. Vijay, J. D. Sau, M. L. Cohen, and I. Siddiqi, "Optimizing anharmonicity in nanoscale weak link josephson junction oscillators," *Phys. Rev. Lett.* **103**, 087003 (2009).
- ²¹Alexey Bezryadin, *Superconductivity in Nanowires: Fabrication and Quantum Transport* (Wiley-VCH Verlag GmbH & Co. KGaA, Leipzig, Weinheim, Singapore, 2012).
- ²²I. Nazhestkin *et al.*, "High kinetic inductance in platinum-coated aluminum nanobridge interferometers," *Advanced Engineering Materials* **27**, 2402385 (2025).
- ²³K. K. Likharev, "Superconducting weak links," *Rev. Mod. Phys.* **51**, 101–159 (1979).
- ²⁴J. Koch, T. M. Yu, J. Gambetta, A. A. Houck, D. I. Schuster, J. Majer, A. Blais, M. H. Devoret, S. M. Girvin, and R. J. Schoelkopf, "Charge-insensitive qubit design derived from the cooper pair box," *Phys. Rev. A* **76**, 042319 (2007).
- ²⁵C. Sun and A. Bezryadin, "Multiple-nanowire superconducting quantum interference devices: critical currents, symmetries, and vorticity stability regions," *Nano Express* **6**, 035014 (2025).
- ²⁶A. A. Golubov, M. Y. Kupriyanov, and E. Il'ichev, "The current-phase relation in josephson junctions," *Rev. Mod. Phys.* **76**, 411–469 (2004).